

Synthesis of highly efficient multivalent disaccharide/[60]fullerene nanoballs for emergent viruses.

Javier Ramos-Soriano,^{§,†} José J. Reina,^{†,||} Beatriz M. Illescas,^{§,*} Noelia de la Cruz,[†] Laura Rodríguez-Pérez,[§] Fátima Lasala,[‡] Javier Rojo,^{†,*} Rafael Delgado,^{‡,*} Nazario Martín^{§,#,*}

[§]Departamento de Química Orgánica, Facultad de Química, Universidad Complutense, 28040 Madrid, Spain; [†] Glycosystems Laboratory, Instituto de Investigaciones Químicas (IIQ), CSIC – Universidad de Sevilla, Av. Américo Vespucio 49, Seville 41092 Spain; [‡]Laboratorio de Microbiología Molecular, Instituto de Investigación Hospital 12 de Octubre (imas12) 28041 Madrid, Spain; [#] IMDEA-Nanoscience, Campus Cantoblanco, 28049 Madrid, Spain.

ABSTRACT: After the last epidemic of Zika virus (ZIKV) in Brazil that peaked in 2016, it has been demonstrated growing evidence of the link between this teratogenic flavivirus and microcephaly cases. However, no vaccine or antiviral drug has been yet approved. ZIKV and Dengue virus (DENV) entry to the host cell takes place through several receptors including DC-SIGN (dendritic cell-specific intercellular adhesion molecule-3-grabbing nonintegrin), so that the blockade of this receptor through multivalent glycoconjugates supposes a promising biological target to inhibit the infection process. In order to get enhanced multivalency in biocompatible systems, tridecafullerenes appended with up to 360 1,2-mannobiosides have been synthesized using a strain promoted cycloaddition of azides to alkynes (SPAAC) strategy. These systems have been tested against ZIKV and DENV infection, showing an outstanding activity in the picomolar range.

INTRODUCTION

The infection of humans by emergent and potentially highly pathogenic agents such as Ebola, Dengue and Zika has not been properly addressed so far. In particular, there are no approved vaccines or specific treatment for Zika virus (ZIKV) infection and, as the evidence of the teratogenic effects of Zika increases, it is more necessary to investigate in antiviral and preventive strategies to counteract its devastating potential.¹ The social and economic costs of the recent spread of ZIKV in Latin America and the Caribbean will total an estimated US\$7-18 billion between 2015 and 2017 (United Nations Development Program).

ZIKV is a positive single-strand RNA virus transmitted by mosquito of the *Aedes* genus during epidemic spread and from human to human by vertical transmission (pregnant women to fetuses) and also through sexual contact since ZIKV is present at high concentrations in semen and genital fluids during and after symptomatic infection.² Amazingly, the infective process of ZIKV is largely unknown. However, in experiments with human skin cells, it appears that ZIKV uses C-type lectin receptor DC-SIGN (dendritic cell-specific intercellular adhesion molecule-3-grabbing non-integrin) among other receptors on host cell surface to enter the cytoplasm by receptor-mediated endocytosis.³ DC-SIGN has been shown to be a significant receptor in the infection and pathogenesis of another flaviviruses such as Dengue virus (DENV).⁴

On the other hand, the interaction of Ebola virus (EBOV) with DC-SIGN in dendritic cells (DCs), and L-SIGN in specific endothelial cells has been reported.⁵ These observations have recently been confirmed in an *in vivo* murine model of EBOV infection in which, after intranasal inoculation of wild type EBOV, the population of DCs expressing DC-SIGN is the first cell subset detected to be infected.⁶ Since DC-SIGN recognizes a special pattern of *N*-linked glycosylation in the envelope glycoprotein of EBOV (high mannose glycans), we have developed some glycoconjugates to block the carbohydrate recognizing domain of DC-SIGN as an antiviral target.⁷ This lectin recognizes mannose and fucose residues from glycoproteins and, typically, a multivalent effect takes place.

A multivalent effect occurs when the binding affinity between the receptor and the multivalent ligand is drastically increased with respect to that found for the monovalent ligand.⁸ Well-designed multivalent inhibitors of infection by different pathogens are interesting weapons to reach strong therapeutic effects and fight current problems as high-dose drugs or drug resistance.⁹ Some multivalent ligands based, for instance, on polymeric, carbon nanotubes or nanoparticle scaffolds have the drawback of the lack of control on the homogeneity of the materials and reproducibility of the synthetic process.¹⁰ However, in the recent years, some so called molecular nanoparticles defined as monodisperse nanometric sized molecular systems with

defined chemical structure have been studied.¹¹ In this context, carbon nanostructures based on well-defined hexakis-adducts of [60]fullerene with octahedral geometry and globular shape have been employed as multivalent scaffolds functionalized with different ligands for a variety of biological applications.¹² In particular, glycofullerenes, hexakis-adducts in which a central [60]fullerene moiety is surrounded by carbohydrate units, have been assayed towards some lectins¹³ as well as glycosidases¹⁴ and glycosyl-transferases,¹⁵ finding interesting therapeutic potential.

In particular, to inhibit the infection by EBOV we have reported some glycofullerenes containing from 12 to 36 mannose units that interact with DC-SIGN showing an important multivalent effect.¹⁶ Moreover, tridecafullerenes containing up to 120 mannose residues have been reported as the most efficient inhibitors of the infection by an artificial EBOV with an IC₅₀ value of 0.66 nM.¹⁷

The synthetic pathway to multivalent ligands usually requires the functionalization of a central multivalent core with several units of the desired functionality.¹⁸ To avoid polydisperse materials, an efficient functionalization process has to be used. In the case of [60]fullerene, hexakis-adducts with octahedral addition pattern are easily obtained by direct cyclopropanation Bingel-Hirsch addition of adequately substituted malonates.¹⁹ We have developed a click chemistry approach based on the preparation of a hexakis-adduct endowed with twelve alkyne moieties to avoid the employ of sterically hindered malonates that leads to low yield syntheses.²⁰ The post-functionalization of those hexakis-adducts can be efficiently and regioselectively carried out by following a copper-catalyzed addition of azides to alkynes (CuAAC) procedure.²¹ This methodology has allowed us to obtain hexakis-adducts of [60]fullerene containing from 12 to 120 monosaccharide units. Further increasing the multivalency of the glycoconjugate is, however, difficult by using this methodology owing to the chelation ability of the carbohydrate units, that complex the copper ion and produces a lowering in the yield of the

process, together with the difficulty to remove the cytotoxic copper after the click reaction.²² To overcome these drawbacks, we have developed a strain promoted cycloaddition of azides to alkynes (SPAAC)²³ strategy by using a cyclooctyne based hexakis-adduct of [60]fullerene.²⁴ This SPAAC building block allows the introduction of azide functionalized glycofullerenes very efficiently by heating the reaction mixture at 50°C under microwave irradiation for 30 min and avoiding the employ of copper, in contrast with the 48 h of reaction needed for a complete functionalization and lower yields obtained by using the CuAAC strategy.

For all the above considerations, we planned the preparation of highly efficient inhibitors of ZIKV and DENV by synthesizing multivalent mannose glycoderivatives built around a biocompatible [60]fullerene scaffold. In order to increase the multivalency of the ligands by keeping at the same time a copper free strategy, we have carried out the synthesis of a new asymmetric cyclooctyne based building block with an azide group at the focal point. This compound has opened the door to groundbreaking tridecafullerenes appended with 120 (**31**) and 360 (**32**) carbohydrate functionalities, in a synthetic step which represents the fastest dendritic growth reported up to now in the literature (Figure 1). Furthermore, as several studies supported that the presence of $\alpha(1,2)$ mannobiosides increases by a factor of 3-4 the affinity of oligosaccharides to DC-SIGN in comparison with the use of mannose,²⁵ we have employed the disaccharide **5** and the glycodendron **8** to functionalize the cyclooctyne-containing building block. It is worth highlighting that these disaccharide derivatives could not have been obtained by using the CuAAC strategy owing to their higher ability of chelating copper between the two monosaccharide units. These unprecedented derivatives have been tested against ZIKV and DENV infection, finding IC₅₀ values for compound **32** endowed with 360 disaccharide moieties in the picomolar range! To the best of our knowledge, these new molecules are the most efficient inhibitors of ZIKV and DENV infections reported so far.

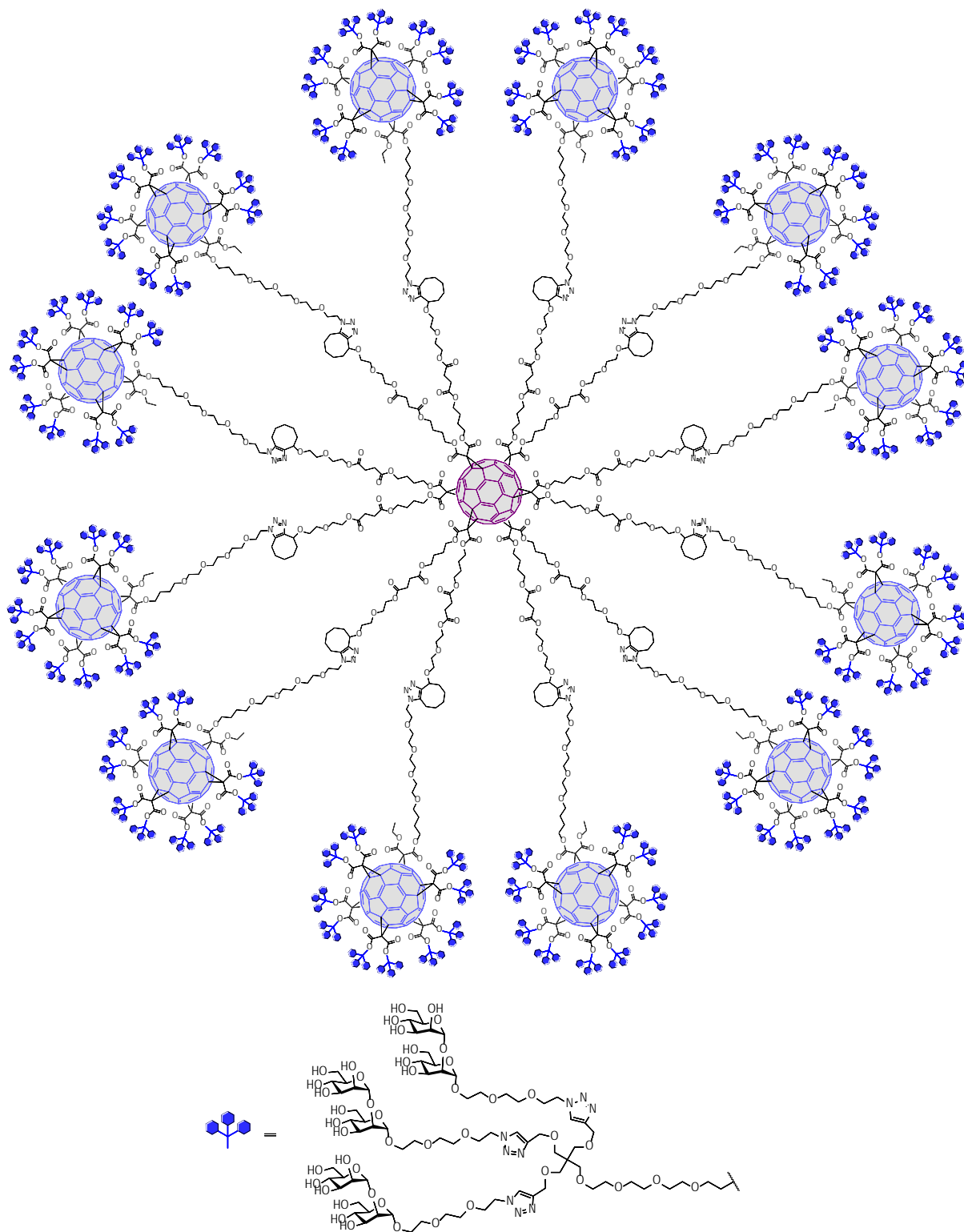


Figure 1. Cartoon representing the tridecafullerene **32** appended with 360 1,2-mannobioside units by using the SPAAC synthetic pathway.

RESULTS AND DISCUSSION

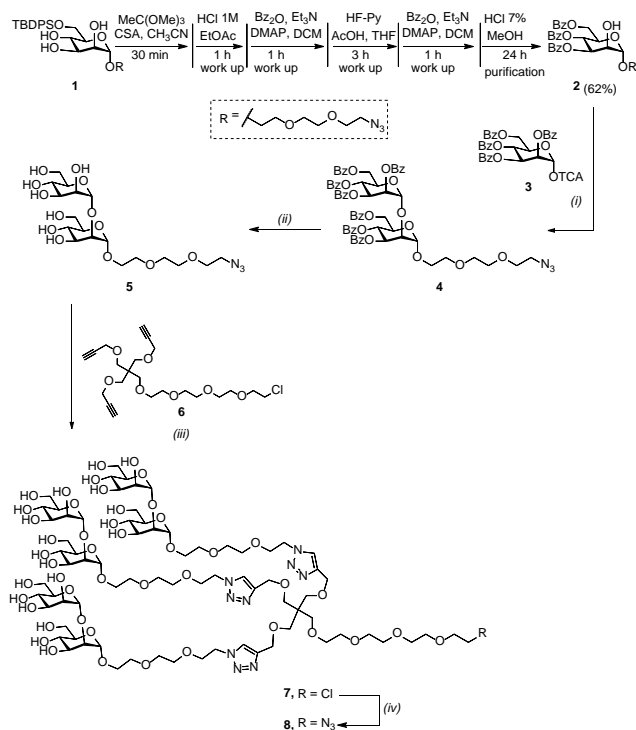
Synthesis.

The synthetic route to obtain mannobioside **5** and glycodendron **8** with an azide in the focal position is depicted in Scheme 1. The synthesis of disaccharide **4** was performed

using the methodology previously reported by some of us to obtain in an efficient manner $\alpha(1-2)$ mannobiosides.²⁶ Applying the “consecutive synthesis” concept, the synthesis of the 2-hydroxy free mannose **2** was performed in six synthetic steps with only one silica gel chromatographic process with 62% yield, starting from the monoprotected

mannoside **1**.²⁷ The disaccharide **4** was prepared by reaction of the glycosyl donor **3**²⁸ with the glycosyl acceptor **2** using trimethylsilyl triflate (TMSOTf) as promoter at 0°C with excellent yield. Finally, the disaccharide **5** was obtained by the deprotection of benzoyl groups using classical Zempler conditions (NaOMe/MeOH) to afford the final compound **5** in excellent yield.

Mannobioside **5** was conjugated to **6**²⁹ by a CuAAC reaction to generate the trivalent intermediate **7** in very good yield after two reaction cycles. The reaction was carried out using CuSO₄ as a copper source, sodium ascorbate to reduce Cu(II) to Cu(I) in situ, and tris[(1-benzyl-1*H*-1,2,3-triazol-4-yl)methyl]amine (TBTA) to stabilize Cu(I). The copper chelating ability of the disaccharides makes it necessary to carry out the reaction a second time to improve the yield on the fully substituted dendrimer **7**. The solution was treated with the Quadrasil MP resin to remove any trace of copper that could cause interferences in the biological assays. Treatment of chloro derivative **7** with sodium azide in DMF at 60°C furnished glycodendrion **8** in excellent yield after Sephadex LH20 purification. The monodispersity and integrity of this glycodendrion were satisfactorily established by both NMR and MS.

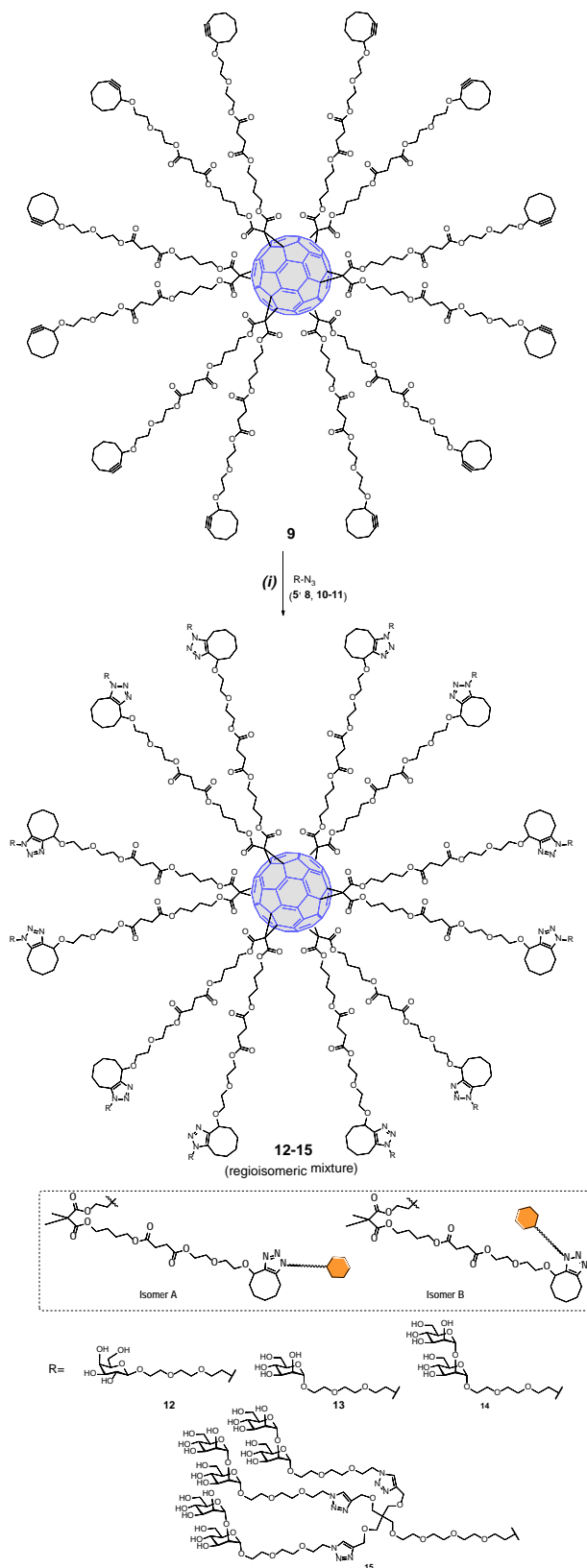


Scheme 1. Reagents and conditions: (i) TMSOTf, DCM, molecular sieves 4 Å, 0°C, 1h (80%); (ii) NaOMe, MeOH, r.t., 2h (94%); (iii) CuSO₄·5H₂O, TBTA, AscNa, DMSO/H₂O (1/1), MW 60°C, 1h (98%), (iv) NaN₃, DMF, 60°C, 3 days (quant.).

To obtain multivalent glycofullerenes we used the cyclooctyne [60]fullerene derivative **9** in order to use the SPAAC click reaction (Scheme 2). Thus, a DMSO solution of cyclooctyne building block **9** and the corresponding azide was heated under microwave irradiation at 50°C for 30 min. For comparison purposes, reaction with galactose and mannose monosaccharides **10-11** was also carried out. By

using this procedure, we obtained the derivatives with 12 monosaccharides (**12-13**) or 12 (**14**) and 36 (**15**) disaccharides. The purification of these multivalent systems was performed by size-exclusion chromatography using Sephadex G-25 leading to the expected products.

Characterization of hexakis adducts **12-15** was performed by FTIR, NMR and XPS. Thus, while the ¹H NMR spectra of these compounds show broadened signals possibly due to intermolecular aggregation, ¹³C NMR allows complete characterization of hexakis-adducts. The signals for the cyclooctyne Csp are very characteristic, which are observed at 110.1 and 92.8 ppm in compound **9**. These signals disappear in the glycofullerenes, thus providing evidence of complete functionalization of the cyclooctyne moieties. Also, the signal of the CH₂ bound to the azido group at ~ 50 ppm is very informative. The disappearance of the signal at 50 ppm coming from the sugar azide indicates that the purification of the compounds has been adequately carried out and the unreacted azide has been removed. Due to the lack of regioselectivity in the thermal cycloaddition to asymmetric cyclooctynes, a mixture of both regioisomers is obtained in all cases, giving rise to duplication of some signals in the NMR spectra. Assignment of these signals was based on COSY and HSQC bidimensional NMR experiments. Thus, for instance, for compound **15** bearing 36 disaccharide units and with two different types of 1,2,3-triazole rings, only two signals for the Csp² of the C₆₀ are observed, as we expected from the hexa-substitution on the [60]fullerene skeleton (δ ~ 140.8 and 145.1) (Figure 2). Also, two signals are observed for the two different carbons of the 36 triazole rings of the glycodendrion moiety (δ ~ 124.1 and 144.0). However, we find two different sets of signals for the triazole rings fused to the cyclooctyne moieties corresponding to the two formed regioisomers (δ ~ 134.4 and 143.8 for the major isomer and δ ~ 133.8 and 143.2 for the minor isomer) (Figure 2).



Scheme 2. Reagents and conditions: (i) DMSO, MW 50°C, 30 min (quant.).

In order to increase the multivalency of the synthesized glycofullerenes while maintaining the copper-free strategy,

an asymmetric $A_{10}B$ macromonomer [60]fullerene derivative bearing 10 cyclooctynes and a chlorine atom at the focal point was prepared according to the procedure represented in Scheme 3. We first prepared monoadduct **21** from the Bingel-Hirsch addition of malonate **20** to [60]fullerene. To obtain the [5:1]-hexa- adduct **23**, an excess of malonate **22** (10 equiv.) and CBr_4 (80 equiv.) were added to a solution of **21** using DBU (20 equiv.) as the base. After deprotection of the hydroxyl groups and esterification with carboxylic acid **25**, the asymmetric compound **26** was obtained.

This asymmetric compound **26** was submitted to the SPAAC reaction under MW irradiation with azide substituted disaccharide **5** and glycodendron **8** yielding the corresponding glycofullerenes **27-28** appended with either ten or thirty disaccharides, respectively, and a chlorine atom at the focal point. These derivatives, after replacement of the chlorine by an azido group, were employed as building blocks to react with the symmetric hexa-adduct **9** leading to giant tridecafullerenes **31-32**, in which a central [60]fullerene scaffold is covalently bound to twelve [60]fullerene units, completely surrounded by carbohydrate moieties. Thus, in one synthetic step we obtained glycofullerenes containing 120 (**31**) or 360 (**32**) disaccharides in an efficient copper-free strategy. Purification of the obtained derivatives **31** and **32** was carried out by ultrafiltration (Amicon® Ultra-15, MWCO 50 kDa and 100 kDa respectively) of a water solution.

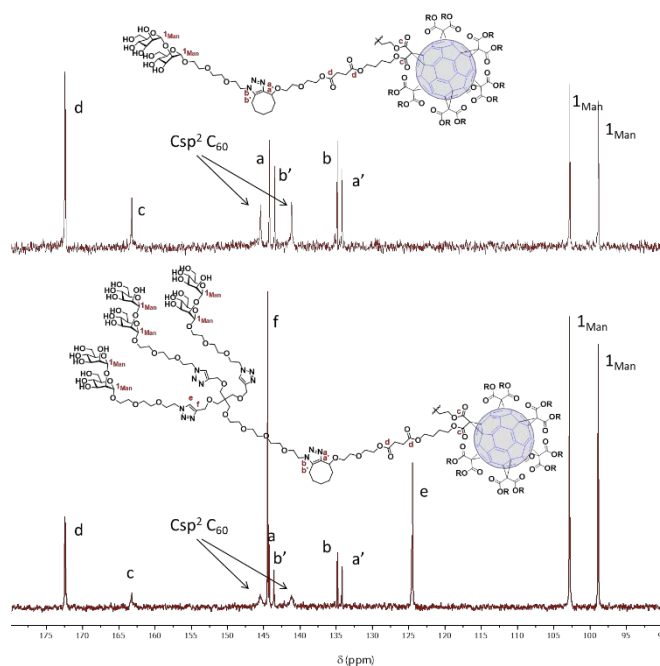
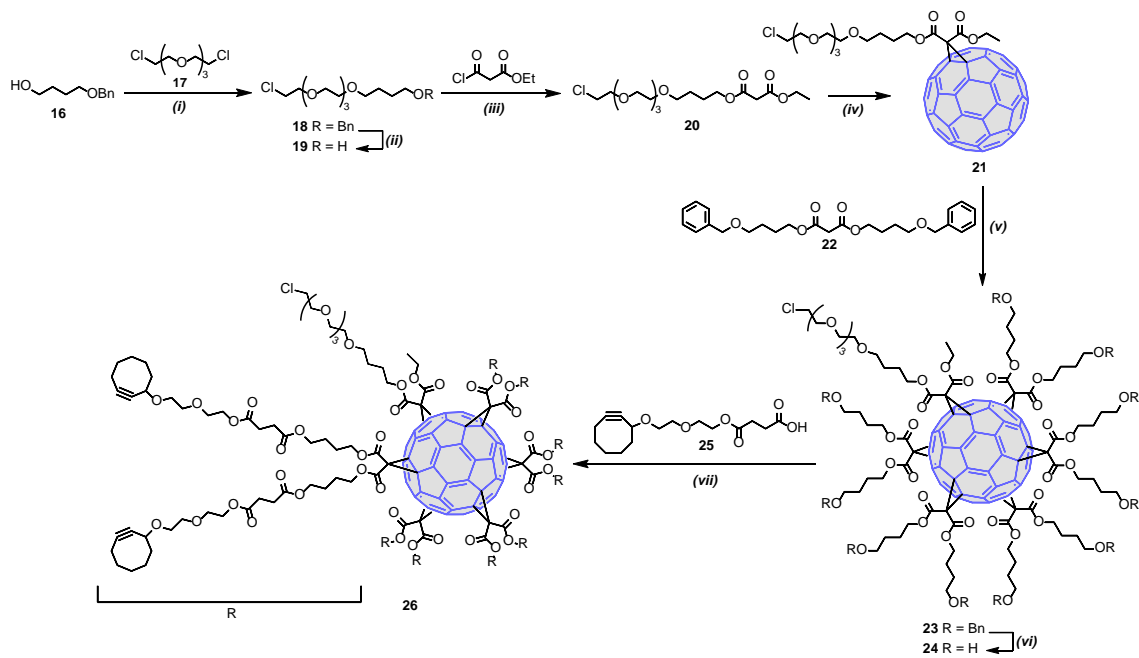
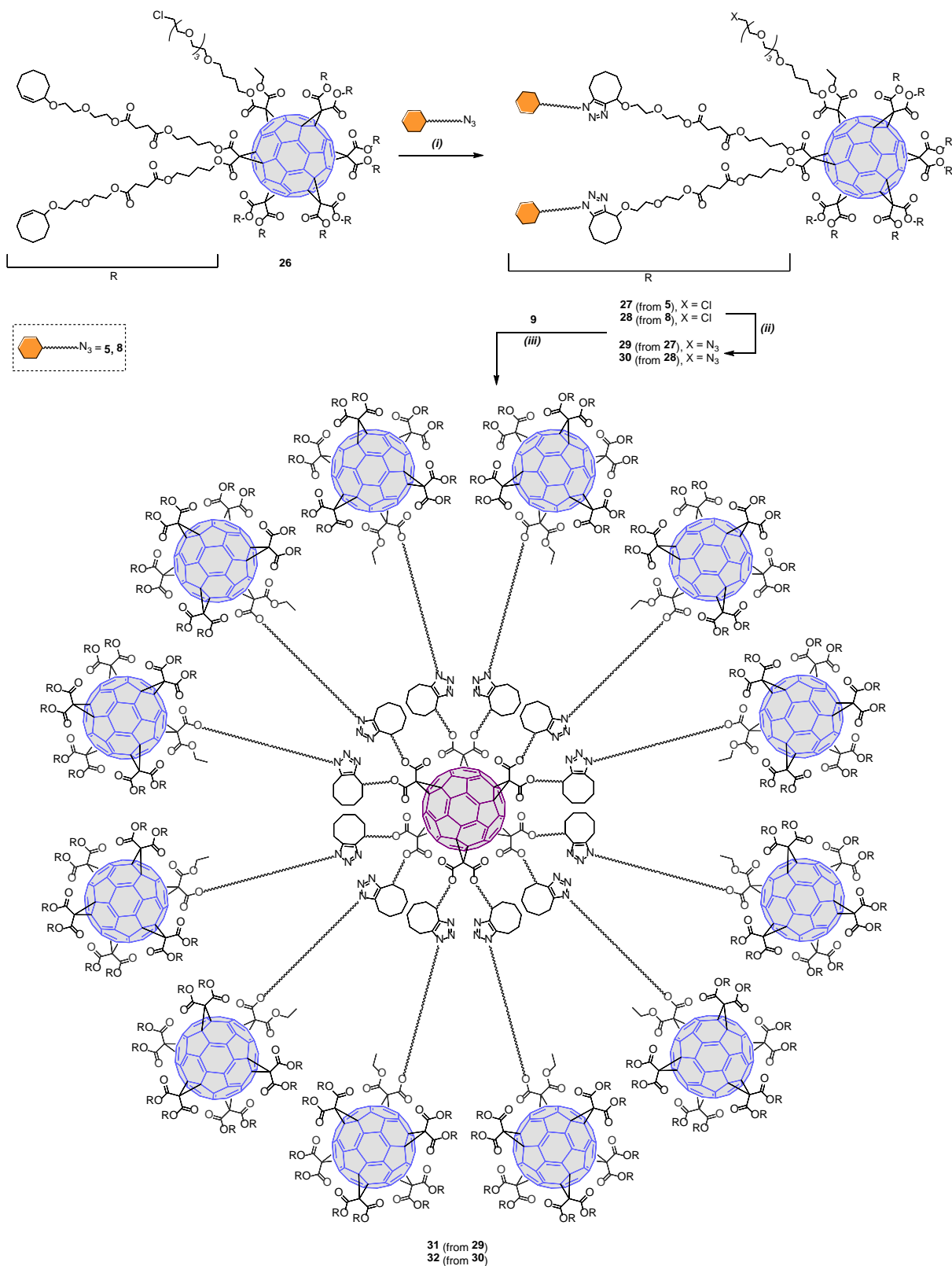


Figure 2. Partial view of the ^{13}C NMR spectra of **14** (up) and **15** (down) ($DMSO-d_6$, 100 MHz).



Scheme 3. Reagents and conditions: (i) TBAHS, NaOH 50%, 45°C, overnight (83%); (ii) H₂, Pd/C, DCM/MeOH (3/1), r.t., 5 h (quant.); (iii) Et₃N, DMAP, dry DCM, r.t., overnight (quant.); (iv) C₆₀, DBU, I₂, dry toluene, 0°C, 4 h (71%); (v) DBU, CBr₄, o-DCB, r.t., 72 h (48%); (vi) H₂, Pd/C, DCM/MeOH (3/1), r.t., overnight (quant.); (vii) DMAP, DCC, dry DCM/DMF (10/1), r.t., overnight (quant.).



Scheme 4. Reagents and conditions: (i) DMSO, MW 50°C, 30 min (quant.); (ii) NaN₃, DMF, 60°C, 3 days (quant.); (iii) DMSO, MW 50°C, 30 min (**31**: 98%, **32**: 94%).

Characterization of these nanoballs was first carried out by FTIR and NMR. Thus, FTIR spectra of **31** and **32** do not show the characteristic signal of the azide group (~ 2126 and 2128 cm⁻¹ in precursors **29** and **30** respectively, see ESI) confirming that the unreacted azide derivatives have been

completely removed in the ultrafiltration process. ¹H NMR spectra of **31-32** show, as previously mentioned, some of the signals duplicated as a consequence of the presence of a mixture of regioisomers resulting from the SPAAC cycloaddition reaction to the cyclooctyne moiety (see ESI). The ¹³C

NMR spectra of these derivatives are, despite the high number of carbon atoms, very representative due to the high symmetry of the compounds. It can be observed that the characteristic signals for the alkyne carbons of the cyclooctyne moiety are not present in the final products **31** and **32**, accounting for the complete functionalization of all the cyclooctynes (Figure 3). For both **31** and **32** only two broadened signals corresponding to the sp^2 carbons of the [60]fullerene are observed ($\delta \sim 140$ and 145). Four signals are encountered for the quaternary carbons of the triazole rings fused to the cyclooctynes, showing the formation of two regioisomers (two signals around 143 ppm and the other two signals around 134 ppm). For derivative **32** other two signals are observed for the two carbons of the triazole ring present in the glycodendrimer ($\delta \sim 124$ and 144).

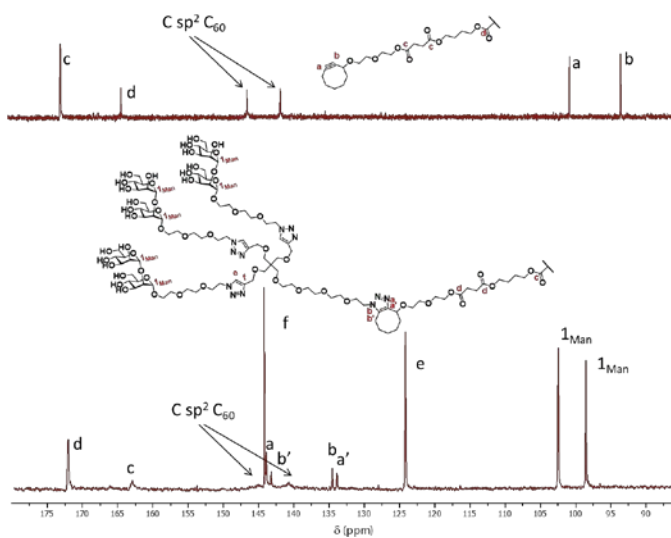


Figure 3. Partial view of the ^{13}C NMR spectra of **26** (up) and **32** (down) ($\text{DMSO-}d_6$, 100 MHz).

While MS spectra of hexakis-adducts **12-14** showed the expected molecular ion peaks ($[\text{M}+\text{Na}]^+$), those for **15** and **31-32** were difficult to obtain and the molecular ion peak could not be clearly observed owing to the very high molecular mass of the compounds and high level of fragmentation arising from both the sugar residues and the Bingel addition pattern on the [60]fullerene sphere.^{14d, 16-17, 30} Therefore, additional characterization by dynamic light scattering (DLS) and X-ray photoelectron spectroscopy (XPS) was carried out.

DLS analyses were carried out in water (2 mg/mL) (Figure 4 and ESI). At this concentration, one or two main size distributions for glycofullerenes **12-15** and **31-32** are observed. The small size distribution is $\sim 6-8.5$ nm for hexa-adducts **12-15** and ~ 11 nm for tridecafullerenes **31-32** and must correspond to only one molecule. It is interesting to note that, in agreement to the introduction of the cyclooctyne moieties with a longer spacer and disaccharides instead of monosaccharides, these sizes are bigger than those observed for the previously reported tridecafullerenes ($\sim 5-6$ nm). The

second size distribution observed for some of the new synthesized compounds varies from 115 to 340 nm and shows the aggregation of several molecules. This aggregation is also observed by the broadening of the signals in the ^1H NMR spectra, thus confirming the existence of a network of intramolecular H-bonds in the observed one-molecule tridecafullerenes as well as intermolecular H-bonds forming the observed aggregates (Figure 4).

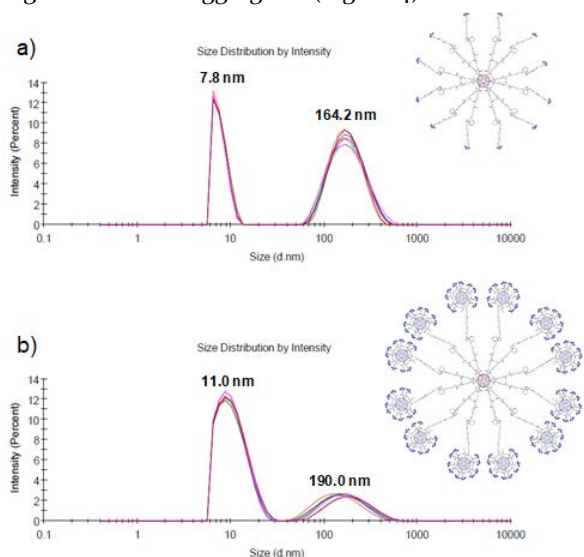


Figure 4. DLS size distribution of a) **15** and b) **32** in water solution.

Further characterization of all new glycofullerenes (**12-15** and **31-32**) was achieved XPS (Figure 5 and ESI). This semi-quantitative surface technique was a valuable tool to gain information about the atoms present in the molecular structure together with their chemical state and relative abundance. Although XPS is not properly a technique to demonstrate the purity of a compound, the data obtained in the XPS survey spectra of the new glycofullerenes (**12-15** and **31-32**) displayed the corresponding peaks of C 1s, O 1s and N 1s with no other spectroscopic signature of impurities, which nicely support the proposed structures. The relative abundance of C, O and N recorded for each sample are in state agreement with the theoretically calculated values (Table S1). Moreover, analyzing the fitting of the high resolution spectra recorded for N 1s, we observed two main components for all glycofullerenes (inserts on Figures 5 and S2-S7). The minor Gaussian-Lorentzian curve centered at higher binding energies was assigned to one nitrogen of the triazole ring while the major peak at lower binding energies to two N atoms bound to C atoms as near neighbours.³¹ It should be highlighted the lack of nitrogen signal at 405 eV which is related to the presence of the azide band, confirming the efficiency of the click reaction forming the triazole ring.

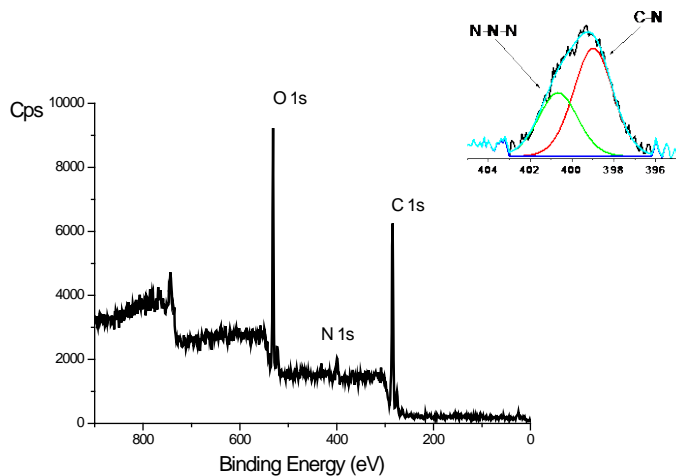


Figure 5. XPS survey spectrum of compound **32** (C_{60} -360ManMan) with the N is deconvoluted components (inset right).

Biological studies

Multiple host cell receptors have been identified to facilitate Flaviviruses entry, including DC-SIGN which interact with Flavivirus envelope proteins (M and E) through their N-glycosylated residues.³² N-glycosylation of viral proteins was shown to affect infection of different viruses, facilitating viral interaction with cellular receptors, or modifying protein immunogenicity and thus changing recognition of the virus by the host immune system. Available data indicate that glycosylation of envelope E glycoprotein is associated with increased infectivity and proper release of mature viral particles and plays an important role in assembly of infective particles, cellular attachment, tropism, transmission and pathogenesis.³³ Although the number of N-glycosylation sites of the envelope of ZIKV and DENV is lower than in the glycoprotein of HIV or EBOV, only 4 in comparison to 18-20, the role of these N-glycosylation residues seems to be important for infectivity.³⁴

DC-SIGN recognizes mannosylated and fucosylated oligosaccharides presented in a multivalent manner on the surface of several pathogens. Thus the preparation of multivalent carbohydrate systems is necessary for the efficient interaction with this receptor as well as for the effective competition with the natural ligands. Therefore, DC-SIGN can function as a good model for studying the first steps of pathogenesis of Flaviviruses and screening the antiviral strategies based on DC-SIGN targeting compounds for vaccination and treatment purposes. In this respect glyco-dendrimeric scaffolds have been shown to achieve antiviral

activity at the μM range against DENV.³⁵ DC-SIGN specific targeting for blocking ZIKV infection has not been explored so far and it is important to assess the potential antiviral capability of interfering with the very first steps of the infective process of ZIKV with novel experimental approaches.

In this study, we have evaluated the inhibitory effect of multivalent disaccharide/fullerene nanoballs in the experiment of direct infection of Jurkat DC-SIGN⁺ with pseudotyped viral particles presenting ZIKV or DENV virus glycoproteins. These globular multivalent systems are water soluble and show no cytotoxicity in cell lines allowing the study of their potential biological function in preventing viral infection (Figure S9). The efficiency of these multivalent compounds to inhibit DC-SIGN mediated infection of ZIKV and DENV through blocking of DC-SIGN was studied in 6 independent experiments. As a control, infection with the DC-SIGN-independent VSV glycoprotein-pseudotyped lentiviral particles was performed in the same conditions.

The results obtained in the infection experiment revealed the dependence of the inhibition effect on mannoses. For the initial testing of compounds, a screening threshold of IC_{50} was set up at $1 \mu\text{M}$ (Figure S8). Compound **12** displaying 12 galactoses, as expected, was not able to inhibit the infection process mediated by DC-SIGN (Figure S8).

Antiviral activity of compounds **15**, **31** and **32**, designed to present 36, 120 or 360 $\alpha(1,2)$ mannobioside residues respectively were thus further characterized. They showed very strong antiviral activity at picomolar to nanomolar concentrations (Figure 6 and Table S2). Compound **15** could effectively block Zika and Dengue virus infection at low nanomolar concentrations with the IC_{50} of 8.35 nM (95%CI = 4.8 - 14.5 nM) for ZIKV and IC_{50} of 7.71 nM (95%CI = 4.85 - 12.24 nM) for DENV pseudotypes respectively. Compound **31** was almost one order of magnitude more potent at inhibiting infection showing the IC_{50} of 516 pM (95%CI = 230pM - 1.150 nM) for ZIKV and IC_{50} of 98 pM (95%CI = 45pM - 213 nM) for DENV.

Finally, compound **32**, containing a greater number of mannobiosides (360), shows the greatest inhibitory activity with the IC_{50} of 67 pM (95%CI = 39 pM - 116 pM) for ZIKV and IC_{50} of 35 pM (95%CI = 18 pM - 68 pM) for DENV (Table S2). These results have confirmed the efficiency of these systems to interact with DC-SIGN and to compete with Flavivirus glycoprotein-pseudotyped particles during their entry into target cells and highlight a potent mechanism for antiviral design to specific receptors based on recognition of carbohydrates.

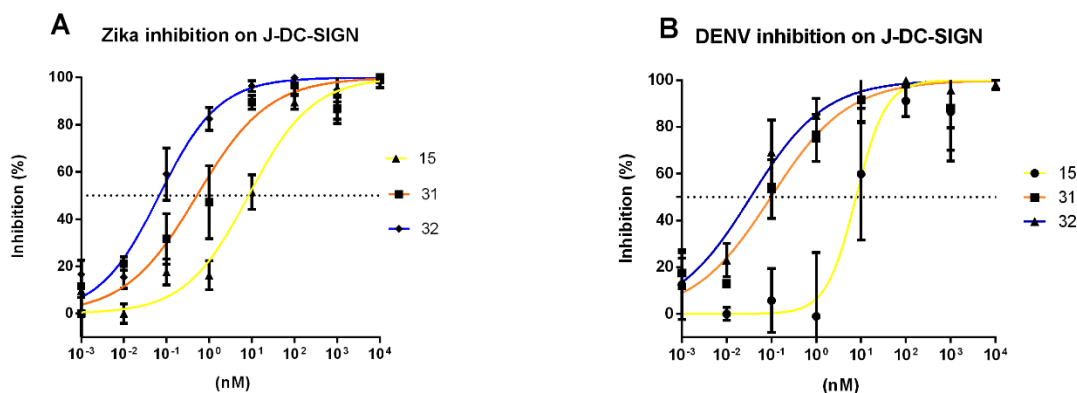


Figure 6. Sensitivity of (A) Zika-Paraiba and (B) DENV-1 virus transduction to the DC-SIGN inhibitors **15**, **31** and **32**.

Conclusions

By using a copper-free strategy based on the SPAAC click-chemistry procedure, unprecedented tridecafullerenes bearing up to 360 disaccharide residues (compound **32**) have been synthesized and characterized. It is important to note that the presence of disaccharides significantly increases the biological activity when compared with previously published monosaccharides. Such compounds could not have been obtained by following a CuAAC methodology owing to the chelating ability of the mannobiosides, making it difficult the complete functionalization of the alkyne appended fullerene scaffold. Although some aggregation is observed by DLS, the new hexakis-adducts, including groundbreaking “giant” molecule **32** having 41.370 atoms (C, H, O, N) is totally soluble in water, thus allowing its use for biomedical purposes.

Characterization of these new hexakis adducts **12-15** and **31-32** was performed by FTIR, ^1H and ^{13}C NMR, DLS and XPS. Thus, whereas the ^1H NMR spectra of these compounds show broadened signals possibly due to intermolecular aggregation, ^{13}C NMR allows complete characterization of hexakis-adducts based on the simplification of the spectra as a consequence of the octahedral symmetry of the respective hexakis adducts. Actually, the observed clean spectra precludes the existence of other multiadducts intermediates in the final products. This conclusion is also based on the lack of nitrogen signal at 405 eV in the XPS spectra, which is related to the presence of the azide band, thus confirming the efficiency of the click reaction affording the triazole ring.

As DC-SIGN is one of the receptors intervening in the entry of ZIKV and DENV into the cells, the employ of the new multivalent hexakis adduct glycofullerenes appended with mannobiosides to block this receptor offers a new strategy to inhibit the viral infection process. Compound **32**, with 360 disaccharide functionalities appended on a tridecafullerene scaffold, shows the best IC_{50} value, which is in the picomolar range for both ZIKV and DENV. As there is not

a specific antiviral therapy against ZIKV currently available, the highly efficient inhibitors of viral infection reported here open the door to the design of new antivirals based on the blockade of carbohydrate receptors.

ACKNOWLEDGMENT

Financial support by the European Research Council (ERC-2012-ADG_20120216 (Chirallcarbon)), European Commission (VIRUSCAN FETPROACT-2016: 731868 – Horizon 2020 Framework Programme), Ministerio de Economía y Competitividad (MINECO) of Spain (projects CTQ2017-84327-P, CTQ2017-83531-R, CTQ2014-52328-P and CTQ2017-86265-P) and Instituto de Salud Carlos III (ISCIII) (FIS PI1400708 and PI1801007) is acknowledged.

ASSOCIATED CONTENT

Supporting Information.

Experimental and spectroscopical data. DLS, XPS, biological assays.

AUTHOR INFORMATION

Corresponding Author

beti@ucm.es
 nazmar@quim.ucm.es
 javier.rojo@iiq.csic.es
 rafael.delgado@salud.madrid.org

ORCID

Beatriz M. Illescas: 0000-0002-4727-8291
 Nazario Martín: 0000-0002-5355-1477
 Javier Rojo: 0000-0003-3173-3437
 Rafael Delgado: 0000-0002-6912-4736

Present Addresses

§ Singular Research Centre in Chemical Biology and Molecular Materials (CIQUS), Organic Chemistry Department, University of Santiago de Compostela (USC), 15782 Santiago de Compostela, Spain.

REFERENCES

1. (a) Petersen, L. R.; Jamieson, D. J.; Honein, M. A., Zika Virus. *N. Engl. J. Med.* **2016**, *375* (3), 294-5; (b) Vogel, G., One year later, Zika scientists prepare for a long war. *Science* **2016**, *354* (6316), 1088-1089.
2. Paz-Bailey, G.; Rosenberg, E. S.; Doyle, K.; Munoz-Jordan, J.; Santiago, G. A.; Klein, L.; Perez-Padilla, J.; Medina, F. A.; Waterman, S. H.; Gubern, C. G.; Alvarado, L. I.; Sharp, T. M., Persistence of Zika Virus in Body Fluids - Final Report. *N. Engl. J. Med.* **2018**, *379* (13), 1234-1243.
3. Hamel, R.; Dejarnac, O.; Wichit, S.; Ekchariyawat, P.; Neyret, A.; Luplertlop, N.; Perera-Lecoin, M.; Surasombatpattana, P.; Talignani, L.; Thomas, F.; Cao-Lormeau, V. M.; Choumet, V.; Briant, L.; Despres, P.; Amara, A.; Yssel, H.; Misse, D., Biology of Zika Virus Infection in Human Skin Cells. *J. Virol.* **2015**, *89* (17), 8880-96.
4. Perera-Lecoin, M.; Meertens, L.; Carnec, X.; Amara, A., Flavivirus entry receptors: an update. *Viruses* **2013**, *6* (1), 69-88.
5. Alvarez, C. P.; Lasala, F.; Carrillo, J.; Muñoz, O.; Corbí, A. L.; Delgado, R., C-Type Lectins DC-SIGN and L-SIGN Mediate Cellular Entry by Ebola Virus in cis and in trans. *J. Virol.* **2002**, *76* (13), 6841-6844.
6. Ludtke, A.; Ruibal, P.; Wozniak, D. M.; Pallasch, E.; Wurr, S.; Bockholt, S.; Gomez-Medina, S.; Qiu, X.; Kobinger, G. P.; Rodriguez, E.; Gunther, S.; Krasemann, S.; Idoyaga, J.; Oestereich, L.; Muñoz-Fontela, C., Ebola virus infection kinetics in chimeric mice reveal a key role of T cells as barriers for virus dissemination. *Sci. Rep.* **2017**, *7*, 43776.
7. Illescas, B. M.; Rojo, J.; Delgado, R.; Martín, N., Multivalent Glycosylated Nanostructures To Inhibit Ebola Virus Infection. *J. Am. Chem. Soc.* **2017**, *139* (17), 6018-6025.
8. Mammen, M.; Choi, S.-K.; Whitesides, G. M., Polyvalent Interactions in Biological Systems: Implications for Design and Use of Multivalent Ligands and Inhibitors. *Angew. Chem. Int. Ed.* **1998**, *37* (20), 2754-2794.
9. Bhatia, S.; Camacho, L. C.; Haag, R., Pathogen Inhibition by Multivalent Ligand Architectures. *J. Am. Chem. Soc.* **2016**, *138* (28), 8654-8666.
10. (a) Imberty, A.; Chabre, Y. M.; Roy, R., Glycomimetics and Glycodendrimers as High Affinity Microbial Anti-adhesins. *Chem. Eur. J.* **2008**, *14* (25), 7490-7499; (b) Roy, R., A Decade of Glycodendrimer Chemistry. *Trends Glycosci. Glycotechnol.* **2003**, *15* (85), 291-310; (c) Roy, R.; Baek, M.-G., Glycodendrimers: novel glycotope isosteres unmasking sugar coding. Case study with T-antigen markers from breast cancer MUC1 glycoprotein. *Rev. Mol. Biotechnol.* **2002**, *90* (3-4), 291-309; (d) Chabre, Y. M.; Roy, R., Chapter 6 - Design and Creativity in Synthesis of Multivalent Neoglycoconjugates. In *Adv. Carbohydr. Chem. Biochem.*, Derek, H., Ed. Academic Press: 2010; Vol. Volume 63, pp 165-393; (e) Cecioni, S.; Imberty, A.; Vidal, S., Glycomimetics versus Multivalent Glycoconjugates for the Design of High Affinity Lectin Ligands. *Chem. Rev.* **2015**, *115* (1), 525-561; (f) Rodríguez-Pérez, L.; Ramos-Soriano, J.; Pérez-Sánchez, A.; Illescas, B. M.; Muñoz, A.; Luczkowiak, J.; Lasala, F.; Rojo, J.; Delgado, R.; Martín, N., Nanocarbon-Based Glycoconjugates as Multivalent Inhibitors of Ebola Virus Infection. *J. Am. Chem. Soc.* **2018**, *140* (31), 9891-9898; (g) Reichardt, N. C.; Martín-Lomas, M.; Penades, S., Opportunities for glyconanomaterials in personalized medicine. *Chem. Commun.* **2016**, *52* (92), 13430-13439.
11. Jiménez Blanco, J. L.; Benito, J. M.; Ortiz Mellet, C.; García Fernández, J. M., Molecular nanoparticle-based gene delivery systems. *J. Drug Deliv. Sci. Technol.* **2017**, *42*, 18-37.
12. Nierengarten, J. F., Fullerene hexa-adduct scaffolding for the construction of giant molecules. *Chem. Commun.* **2017**, *53* (87), 11855-11868.
13. (a) Sánchez-Navarro, M.; Muñoz, A.; Illescas, B. M.; Rojo, J.; Martín, N., [60]Fullerene as Multivalent Scaffold: Efficient Molecular Recognition of Globular Glycofullerenes by Concanavalin A. *Chem. Eur. J.* **2011**, *17* (3), 766-769; (b) Durka, M.; Buffet, K.; Iehl, J.; Holler, M.; Nierengarten, J.-F.; Taganna, J.; Bouckaert, J.; Vincent, S. P., The functional valency of dodecamannosylated fullerenes with *Escherichia coli* FimH-towed novel bacterial antiadhesives. *Chem. Commun.* **2011**, *47* (4), 1321-1323; (c) Buffet, K.; Gillon, E.; Holler, M.; Nierengarten, J. F.; Imberty, A.; Vincent, S. P., Fucofullerenes as tight ligands of RSL and LecB, two bacterial lectins. *Org. Biomol. Chem.* **2015**, *13* (23), 6482-92.
14. (a) Compain, P.; Decroocq, C.; Iehl, J.; Holler, M.; Hazeldard, D.; Mena-Barragán, T.; Ortiz-Mellet, C.; Nierengarten, J.-F., Glycosidase Inhibition with Fullerene Iminosugar Balls: A Dramatic Multivalent Effect. *Angew. Chem.* **2010**, *122* (33), 5889-5892; (b) Nierengarten, J. F.; Schneider, J. P.; Trinh, T. M. N.; Joosten, A.; Holler, M.; Lepage, M. L.; Bodlenner, A.; Garcia-Moreno, M. I.; Ortiz Mellet, C.; Compain, P., Giant Glycosidase Inhibitors: First- and Second-Generation Fullerodendrimers with a Dense Iminosugar Shell. *Chem. Eur. J.* **2018**, *24* (10), 2483-2492; (c) Abellan Flos, M.; García Moreno, M. I.; Ortiz Mellet, C.; García Fernández, J. M.; Nierengarten, J. F.; Vincent, S. P., Potent Glycosidase Inhibition with Heterovalent Fullerenes: Unveiling the Binding Modes Triggering Multivalent Inhibition. *Chem. Eur. J.* **2016**, *22* (32), 11450-60; (d) Trinh, T. M. N.; Holler, M.; Schneider, J. P.; García-Moreno, M. I.; García Fernández, J. M.; Bodlenner, A.; Compain, P.; Ortiz Mellet, C.; Nierengarten, J.-F., Construction of giant glycosidase inhibitors from iminosugar-substituted fullerene macromonomers. *J. Mater. Chem. B* **2017**, *5* (32), 6546-6556.
15. Tikad, A.; Fu, H.; Sevrain, C. M.; Laurent, S.; Nierengarten, J. F.; Vincent, S. P., Mechanistic Insight into Heptosyltransferase Inhibition by using Kdo Multivalent Glycoclusters. *Chem. Eur. J.* **2016**, *22* (37), 13147-55.
16. Luczkowiak, J.; Muñoz, A.; Sánchez-Navarro, M.; Ribeiro-Viana, R.; Ginieis, A.; Illescas, B. M.; Martín, N.; Delgado, R.; Rojo, J., Glycofullerenes Inhibit Viral Infection. *Biomacromolecules* **2013**, *14* (2), 431-437.
17. Muñoz, A.; Sigwalt, D.; Illescas, B. M.; Luczkowiak, J.; Rodríguez-Pérez, L.; Nierengarten, I.; Holler, M.; Remy, J.-S.; Buffet, K.; Vincent, S. P.; Rojo, J.; Delgado, R.; Nierengarten, J.-F.; Martín, N., Synthesis of giant globular multivalent glycofullerenes as potent inhibitors in a model of Ebola virus infection. *Nat Chem* **2016**, *8* (1), 50-57.
18. Kanfar, N.; Bartolami, E.; Zelli, R.; Marra, A.; Winum, J.-Y.; Ulrich, S.; Dumy, P., Emerging trends in enzyme inhibition by multivalent nanoconstructs. *Org. Biomol. Chem.* **2015**, *13* (39), 9894-9906.
19. Hirsch, A., Principles of Fullerene Reactivity. In *Fullerenes and Related Structures*, Hirsch, A., Ed. Springer Berlin Heidelberg: 1999; Vol. 199, pp 1-65.
20. Nierengarten, J.-F.; Iehl, J.; Oerthel, V.; Holler, M.; Illescas, B. M.; Munoz, A.; Martín, N.; Rojo, J.; Sánchez-Navarro, M.; Cecioni, S.; Vidal, S.; Buffet, K.; Durka, M.; Vincent, S. P., Fullerene sugar balls. *Chem. Commun.* **2010**, *46* (22), 3860-3862.
21. Nierengarten, I.; Nierengarten, J. F., The impact of copper-catalyzed alkyne-azide 1,3-dipolar cycloaddition in fullerene chemistry. *Chem. Rec.* **2015**, *15* (1), 31-51.
22. Ornelas, C.; Broichhagen, J.; Weck, M., Strain-Promoted Alkyne Azide Cycloaddition for the Functionalization of Poly(amide)-Based Dendrons and Dendrimers. *J. Am. Chem. Soc.* **2010**, *132* (11), 3923-3931.
23. (a) Agard, N. J.; Prescher, J. A.; Bertozzi, C. R., A Strain-Promoted [3 + 2] Azide-Alkyne Cycloaddition for Covalent Modification of Biomolecules in Living Systems. *J. Am. Chem. Soc.* **2004**, *126* (46), 15046-15047; (b) Agard, N. J.; Baskin, J. M.; Prescher, J. A.; Lo, A.; Bertozzi, C. R., A Comparative Study of Bioorthogonal Reactions with Azides. *ACS Chem. Biol.* **2006**, *1* (10), 644-648; (c) Baskin, J. M.; Prescher, J. A.; Laughlin, S. T.;

- Agard, N. J.; Chang, P. V.; Miller, I. A.; Lo, A.; Codelli, J. A.; Bertozzi, C. R., Copper-free click chemistry for dynamic in vivo imaging. *Proc. Nat. Acad. Sci. USA* **2007**, *104* (43), 16793-16797.
24. Ramos-Soriano, J.; Reina, J. J.; Perez-Sanchez, A.; Illescas, B. M.; Rojo, J.; Martin, N., Cyclooctyne [60]fullerene hexakis adducts: a globular scaffold for copper-free click chemistry. *Chem. Commun.* **2016**, *52* (69), 10544-10546.
25. (a) Feinberg, H.; Castelli, R.; Drickamer, K.; Seeberger, P. H.; Weis, W. I., Multiple modes of binding enhance the affinity of DC-SIGN for high mannose N-linked glycans found on viral glycoproteins. *J. Biol. Chem.* **2007**, *282* (6), 4202-9; (b) Feinberg, H.; Mitchell, D. A.; Drickamer, K.; Weis, W. I., Structural basis for selective recognition of oligosaccharides by DC-SIGN and DC-SIGNR. *Science* **2001**, *294* (5549), 2163-6; (c) Thépaut, M.; Guzzi, C.; Sutkeviciute, I.; Sattin, S.; Ribeiro-Viana, R.; Varga, N.; Chabrol, E.; Rojo, J.; Bernardi, A.; Angulo, J.; Nieto, P. M.; Fieschi, F., Structure of a Glycomimetic Ligand in the Carbohydrate Recognition Domain of C-type Lectin DC-SIGN. Structural Requirements for Selectivity and Ligand Design. *J. Am. Chem. Soc.* **2013**, *135* (7), 2518-2529.
26. (a) Reina, J. J.; Di Maio, A.; Ramos-Soriano, J.; Figueiredo, R. C.; Rojo, J., Rapid and efficient synthesis of α (1-2)mannobiosides. *Org. Biomol. Chem.* **2016**, *14* (10), 2873-2882; (b) Ramos-Soriano, J.; de la Fuente, M. C.; de la Cruz, N.; Figueiredo, R. C.; Rojo, J.; Reina, J. J., Straightforward synthesis of Mang, the relevant epitope of the high-mannose oligosaccharide. *Org. Biomol. Chem.* **2017**, *15* (42), 8877-8882.
27. Imai, Y.; Hirono, S.; Matsuba, H.; Suzuki, T.; Kobayashi, Y.; Kawagishi, H.; Takahashi, D.; Toshima, K., Degradation of target oligosaccharides by anthraquinone-lectin hybrids with light switching. *Chem. Asian J.* **2012**, *7* (1), 97-104.
28. Hartmann, M.; Betz, P.; Sun, Y.; Gorb, S. N.; Lindhorst, T. K.; Krueger, A., Saccharide-modified nanodiamond conjugates for the efficient detection and removal of pathogenic bacteria. *Chem. Eur. J.* **2012**, *18* (21), 6485-92.
29. Ribeiro-Viana, R.; Sánchez-Navarro, M.; Luczkowiak, J.; Koeppe, J. R.; Delgado, R.; Rojo, J.; Davis, B. G., Virus-like glycodendrinanoparticles displaying quasi-equivalent nested polyvalency upon glycoprotein platforms potently block viral infection. *Nat. Commun.* **2012**, *3*, 1303.
30. Sigwalt, D.; Caballero, R.; Holler, M.; Strub, J.-M.; Van Dorsselaer, A.; Nierengarten, J.-F., Ultra-Fast Dendritic Growth Based on the Grafting of Fullerene Hexa-Adduct Macromonomers onto a Fullerene Core. *Eur. J. Org. Chem.* **2016**, *2016* (16), 2882-2887.
31. Ciampi, S.; Böcking, T.; Kilian, K. A.; James, M.; Harper, J. B.; Gooding, J. J., Functionalization of Acetylene-Terminated Monolayers on Si(100) Surfaces: A Click Chemistry Approach. *Langmuir* **2007**, *23* (18), 9320-9329.
32. (a) Tassaneeritthep, B.; Burgess, T. H.; Granelli-Piperno, A.; Trumfpheller, C.; Finke, J.; Sun, W.; Eller, M. A.; Pattanapanyasat, K.; Sarasombath, S.; Birx, D. L.; Steinman, R. M.; Schlesinger, S.; Marovich, M. A., DC-SIGN (CD209) mediates dengue virus infection of human dendritic cells. *J. Exp. Med.* **2003**, *197* (7), 823-9; (b) Pokidysheva, E.; Zhang, Y.; Battisti, A. J.; Bator-Kelly, C. M.; Chipman, P. R.; Xiao, C.; Gregorio, G. G.; Hendrickson, W. A.; Kuhn, R. J.; Rossmann, M. G., Cryo-EM reconstruction of dengue virus in complex with the carbohydrate recognition domain of DC-SIGN. *Cell* **2006**, *124* (3), 485-93.
33. (a) Davis, C. W.; Nguyen, H. Y.; Hanna, S. L.; Sanchez, M. D.; Doms, R. W.; Pierson, T. C., West Nile virus discriminates between DC-SIGN and DC-SIGNR for cellular attachment and infection. *J. Virol.* **2006**, *80* (3), 1290-301; (b) Beasley, D. W.; Whiteman, M. C.; Zhang, S.; Huang, C. Y.; Schneider, B. S.; Smith, D. R.; Gromowski, G. D.; Higgs, S.; Kinney, R. M.; Barrett, A. D., Envelope protein glycosylation status influences mouse neuroinvasion phenotype of genetic lineage 1 West Nile virus strains. *J. Virol.* **2005**, *79* (13), 8339-47; (c) Hanna, S. L.; Pierson, T. C.; Sanchez, M. D.; Ahmed, A. A.; Murtadha, M. M.; Doms, R. W., N-linked glycosylation of west nile virus envelope proteins influences particle assembly and infectivity. *J. Virol.* **2005**, *79* (21), 13262-74.
34. Mossenta, M.; Marchese, S.; Poggianella, M.; Slon Campos, J. L.; Burrone, O. R., Role of N-glycosylation on Zika virus E protein secretion, viral assembly and infectivity. *Biochem. Biophys. Res. Commun.* **2017**, *492* (4), 579-586.
35. Varga, N.; Sutkeviciute, I.; Ribeiro-Viana, R.; Berzi, A.; Ramdasi, R.; Daggetti, A.; Vettoretti, G.; Amara, A.; Clerici, M.; Rojo, J.; Fieschi, F.; Bernardi, A., A multivalent inhibitor of the DC-SIGN dependent uptake of HIV-1 and Dengue virus. *Biomaterials* **2014**, *35* (13), 4175-84.

Insert Table of Contents artwork here

